

## Direct observation of macromolecular deposition on a nanofiltration membrane

Elina Yachnin and Guy Z. Ramon

Department of Civil and Environmental Engineering, Technion – Israel Institute of Technology, Haifa, Israel

### ABSTRACT

The mechanistic aspects of membrane fouling have been studied extensively using direct observation, but limited to early stages of particulate deposition. Herein, we describe a versatile method extending direct observation to organic fouling, facilitating real-time monitoring of fouling formation and detachment. A transparent gel-like fouling layer is visualized using epi-fluorescent microscopy with the aid of labeled marker beads, trapped at various distances from the membrane, enabling monitoring of variations within the deposit. Fouling and cleaning experiments were conducted, examining alginate deposition and detachment, and illustrating the utility of the proposed method for studying the kinetics of fouling processes.

### ARTICLE HISTORY

Received 7 April 2016  
Accepted 8 August 2016

### KEYWORDS

Fouling; membrane separation; nanofiltration; direct observation

### Introduction

The demand for freshwater is rising rapidly worldwide due to human population growth, climate changes and contamination of existing water resources.<sup>[1]</sup> An increasingly popular solution to water-stress is desalination, in particular by membrane-based processes such as reverse osmosis (RO) and nanofiltration (NF), due to their capacity for highly selective separation and relatively low energy consumption.<sup>[1–3]</sup> However, colloidal particles, mineral precipitates, organic molecules and biofilm-forming bacteria deposit and foul the membrane surface, reducing the permeate flux, increasing energy consumption and reducing process efficiency.<sup>[4,5]</sup> In particular, fouling originating from macromolecular deposition is complex and diverse and its reversibility is influenced by many parameters, such as operational and physico-chemical properties of both feed solution and membrane used; hence, its removal and management is still a challenge and a subject of on-going research.<sup>[4,6–7]</sup>

The study of fouling has been significantly advanced through the use of microscopy, specifically the so-called direct microscopic observation method. Li *et al.*<sup>[8]</sup> were the first to publish a preliminary study of non-invasive, *in situ*, continuous direct observation through the membrane (DOTM) of a particle deposition process. The experimental setup consisted of an optical microscope that observed particle deposition on the surface of a transparent membrane from the permeate side in a cross-flow

microfiltration (CFMF) module during filtration. They examined the dependence of colloid deposition, adhesion and possible re-dispersion on the permeate flux, tangential shear (or cross-flow velocity), particle size and the feed chemistry, using yeast cells and latex beads. This work demonstrated that DOTM is a powerful technique for the fundamental study of deposition and membrane–particle interactions, and further investigations were subsequently carried out.<sup>[9,10]</sup> In a later study, Davis and Mores employed a microscope positioned on the feed side of the membrane channel (termed direct visual observation, or DVO)<sup>[11,12]</sup> for examining yeast deposition and the use of back-pulses for membrane cleaning. Li *et al.*<sup>[13]</sup> further expanded the DOTM method by incorporating it with fluorescence microscopy to observe, *in situ*, the characteristics of cake formation on the membrane surface at the critical flux and above it. Additionally, the study was aimed at assessing the removal of the cake in response to a flux reduction to below the critical value and down to zero.

These past studies not only developed and improved the DOTM method but also provided a qualitative understanding of the various factors that influence biofouling of membrane surfaces. The main factors that control colloid and microbial cell deposition mechanisms are hydrodynamic factors (permeation, cross-flow, back-pulsing), membrane surface properties (hydrophobicity, charge, roughness and pore size), bulk solution chemistry (pH, ionic strength and electrolyte type) and microbial suspension properties (size, number density and microorganism type). Kang *et al.*<sup>[14]</sup>

**CONTACT** Guy Z. Ramon  ramong@technion.ac.il  Department of Civil and Environmental Engineering, Technion – Israel Institute of Technology, Haifa 32000, Israel.

Color versions of one or more of the figures in the article can be found online at [www.tandfonline.com/lsst](http://www.tandfonline.com/lsst).

© 2016 Taylor & Francis

incorporated the direct observation method in an attempt to gain a quantitative understanding of the mechanisms governing initial deposition and release of biocolloids in cross-flow microfiltration processes. Digital image analysis provided temporal data on the membrane surface coverage and the net deposition rate was deduced. Wang *et al.*<sup>[15]</sup> examined a membrane cleaning process using direct observation with ultrafiltration (UF) membranes. Fractional surface coverage was determined while applying back-pulsing – short reversals of the permeate flow direction. This method appeared to be more effective for removing deposited cells than cross-flow shear. The method was then extended further to studies of deposition and release in high-pressure membrane applications such as NF and RO.<sup>[16–18]</sup>

When studying the formation of a fouling layer under flow and high pressure, the flow cells used become inevitably larger and thicker so that optically accessing the formed fouling layer during an experiment becomes challenging. Furthermore, most macromolecular deposits are transparent due to their high water content and require the use of fluorescent labeling. These are some of the difficulties in applying direct observation to macromolecular fouling. Another potential problem is the high variability of the macromolecular substances that cause membrane fouling (*e.g.* biofilm polysaccharides, humic acids, proteins and many more). The treated water will normally contain a mixture of these substances.<sup>[19]</sup> It is possible to use staining techniques for visualizing the various substances, but this method targets specific chemical properties of fouling components and thus some knowledge of the expected composition is required; furthermore, the labelling normally involves binding of the fluorescently tagged ligand, which results in some degree of cross-linking and invariably alters the mechanical properties of the deposit.

Herein, we present a methodology that extends the direct observation method, hitherto only used for initial deposition studies of particulate matter, to study macromolecular fouling. Although the direct observation method is well developed at this point, its main use has been to examine particulate deposition. This deposition is the first stage of fouling development, but it is the formation of a macromolecular fouling layer that triggers the severe reduction of permeate flux. Therefore, direct observation of macromolecular fouling and release will allow a more accurate prediction of the underlying mechanisms occurring at the membrane surface. This knowledge may be used for better informed operational conditions and, possibly, lead to improved membrane design.

## Materials and methods

### Conceptual methodology

This paper shows a proof of concept for an easy and highly versatile method to observe real-time macromolecular fouling and detachment with the aid of fluorescent marker beads. When a solution of examined macromolecules and the markers is introduced to the system, these components will start to deposit on the membrane surface and marker deposition can be monitored through an epi-fluorescent microscope. Schematically, the process may be described as follows: first, the markers deposit directly on the membrane (*Fig. 1a*); after a while, the marker beads' deposition at various distances from the membrane is observed – these beads are trapped in the formed layer and their motion is hindered due to the visco-elastic (or purely viscous) medium (*Fig. 1b*). Once detachment is triggered, the continued presence of these markers serves as an indication of the membrane area where the fouling layer is still intact or, in contrast, where the detachment is already complete (*Fig. 1c*).

The described method enables real-time examination of properties that have not yet been investigated in this context. The thickness of the formed fouling layer can be estimated, indicative of the rate of fouling accumulation under various conditions, and the effectiveness of various cleaning techniques. In this work, sodium alginate salt, a substance that is commonly used to model biofouling, was used. Alginates are linear copolymers which can form a three-dimensional network by ionic cross-links where divalent cations, for example, calcium, bind different alginate chains, inducing the formation of “bridges” between the chains. Alginate studies have shown that increasing the cross-linking density, by addition of calcium ions, increases the stiffness of alginate gels.<sup>[20–23]</sup> Various studies have reported that when an alginate gel layer, cross-linked due to the presence of calcium, is exposed to a sodium chloride solution, ion-exchange between sodium and calcium ions takes place, resulting in the breakup of the alginate gel network.<sup>[24–26]</sup> Analogous to conventional ion exchange processes, the steps involved in sodium chloride cleaning of alginate gel layer are (i) diffusion of sodium ions into the alginate gel layer and (ii) breakup of calcium-alginate bonds by exchanging the calcium with sodium, thereby freeing the alginate molecules to transport away from the loosened fouling layer. Due to these relatively well-understood physico-chemical interactions and ease of manipulation, alginate provides a convenient model system for demonstrating the visualization method.

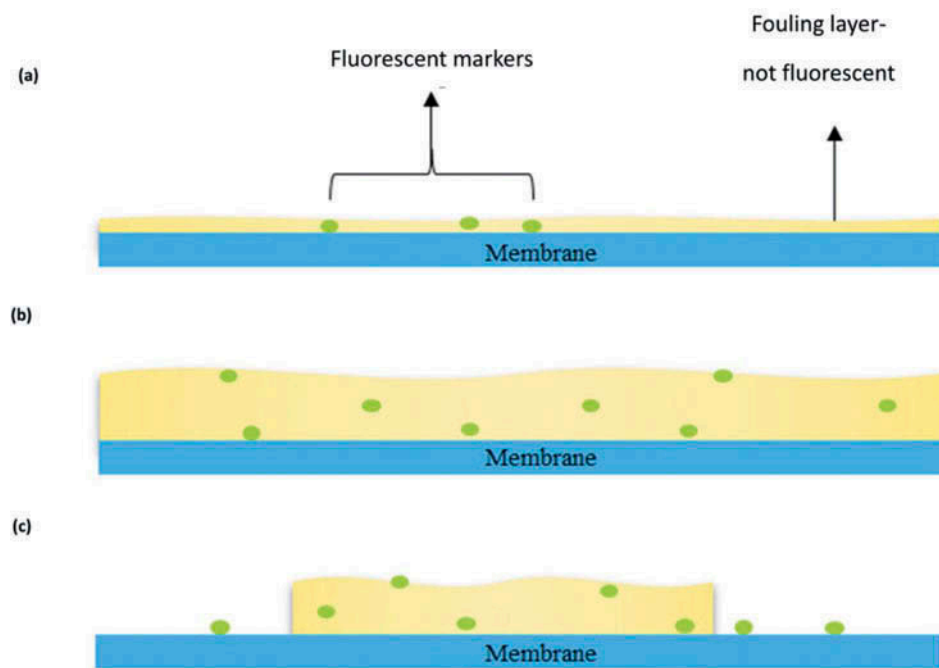


**Figure 1.** Schematic diagram of alginate observation technique at: (a) the beginning and (b) the progress of deposition process and (c) after detachment is triggered.

### Experimental system

A custom-made cross-flow membrane filtration cell was used, fitted with a glass window enabling optical access. Cross-flow channel dimensions within the module are 0.8 mm (height)  $\times$  10 mm (width)  $\times$  21 mm (length) with a total membrane area of  $2.1 \cdot 10^{-4}$  m<sup>2</sup>. The flow cell is mounted on the fixed stage of an epi-fluorescence upright microscope (Leica M5500, Leica Microsystems, Wetzlar, Germany) equipped with a long-working distance, 10 $\times$  objective and a high-sensitivity CCD camera (Clara, Andor, Belfast, Northern Ireland) that allows the acquiring of images in real time during each experiment. The feed stream is continuously stirred and is circulated through the flow cell using a programmable gear pump (Micropump, Cole Parmer, Vernon Hills, IL, USA). Applied pressure is adjusted using a backpressure valve. Permeate volumetric flow rate is measured using an ultra-low flow sensor (Mitos Flow Rate Sensor, Dolomite Ltd., Norwell, MA, USA).

### Feed solution preparation

The feed stream contains a background electrolyte and a fouling component. Sodium chloride or calcium chloride dehydrate (ACS reagent grade, Sigma-Aldrich, St. Louis, MO, USA) at an ionic strength of 10 mM and an unadjusted pH were chosen as the electrolyte. Deionized water was used to prepare all the solutions. Carboxyl-modified, fluorescent-labelled, 1  $\mu$ m diameter polystyrene beads

(FluoSpheres, Life Technologies, (Invitrogen, Ltd.), Paisley, UK) were used as markers. The particles emit blue fluorescence at 415 nm (excitation at 365 nm). The solution provided by the manufacturer contains  $3.1 \times 10^{10}$  particles/mL (2% solid fraction). To avoid contamination of the original solution, it is diluted to a stock solution with a concentration of  $10^8$  particles/mL. The fouling solution is then prepared with a fixed concentration of  $10^6$  particles/mL by further diluting the stock solution. Alginate sodium salt from brown algae (Sigma-Aldrich) was used to model macromolecular fouling. A 10 g/L stock solution was prepared by dissolving 0.5 g of dry alginate powder in 50 mL of deionized water under vigorous stirring. For each fouling experiment this stock solution was added to the feed solution to achieve a concentration of 1 g/L.

### Deposition and release experimental procedure

Each deposition and release experiment followed the same protocol, which begins with deionized water filtration at gradually increased pressure to account for compaction and other sources of flux decline inherent to bench-scale cross-flow membrane filtration systems. Fresh membrane coupons were used at the start of each experiment. The pure water permeability was determined by measuring the permeate flux of deionized water as the pressure was increased gradually. This was followed by filtration of a foulant-free electrolyte solution at a constant pressure, during which both permeate flux and rejection (*i.e.*

permeate salt concentration) were monitored for the clean, compacted membranes. Once the applied pressure was stabilized, the fluorescent particles were added to the feed and the system was monitored while initial particle deposition occurred. Next, alginate was added and the deposition experiment began. During the experiment, permeate flux decline was monitored. Three images from random locations on the membrane surface and cross-sectional ( $z$  axis) images were taken at the beginning and end of each experiment. After each deposition experiment, alginate release was triggered. Two cases were considered: for a feed solution containing sodium ions (as NaCl) the detachment was achieved by shutting off the applied trans-membrane pressure, while in experiments where calcium ions (as  $\text{CaCl}_2$ ) were used as the electrolyte this step was followed by addition of sodium ions to the solution, to induce alginate gel breakup and release. Detachment was monitored for as long as the process was in progress and when no further changes were observed, cross-sectional images were obtained in addition to three images from random locations.

## Results and discussion

### Direct observation of alginate fouling

Representative images of an alginate fouling layer, formed *without* the presence of calcium, are shown in Fig. 2. In this experiment, the feed ionic strength was 10 mM and the permeation rate was  $10 \mu\text{m/s}$ . Images

were taken 15 min after the deposition began. Figure 2a shows the membrane surface, designated as  $z = 0$ , where only the particles that deposited directly on the membrane surface are present. Figure 2b shows the focal plane that is located  $\sim 14 \mu\text{m}$  from the surface of the membrane. In this slice blurry, out-of-focus particles that are deposited on the membrane can still be seen together with new, focused particles. In Fig. 2c another focal plane is shown, located  $\sim 25 \mu\text{m}$  from the membranes' surface. Here, the particles that deposited on the membrane are completely out-of-focus and the particles of the second focal plane are blurry. These images are representative of what forms the basis of our method for macromolecular visualization.

A particularly noticeable attribute of alginate layers formed in the absence of calcium is their fluidity, as they retain a purely viscous characteristic. Away from the membrane surface, marker beads may be seen drifting very slowly, at an increasing rate which abruptly increases upon leaving the alginate layer. This transition is the main determinant for estimating the thickness of the alginate layer. In contrast, in the layers formed in the presence of calcium, the marker beads are immobilized and their drift, if present, is extremely small. Image analysis of particle drift may be used, in principle, to infer rheological properties of these layers, and is the focus of on-going work.

Unlike reported experiments where visualization of particle deposition was aimed at revealing kinetics, in the alginate deposition experiments fouling is significant and

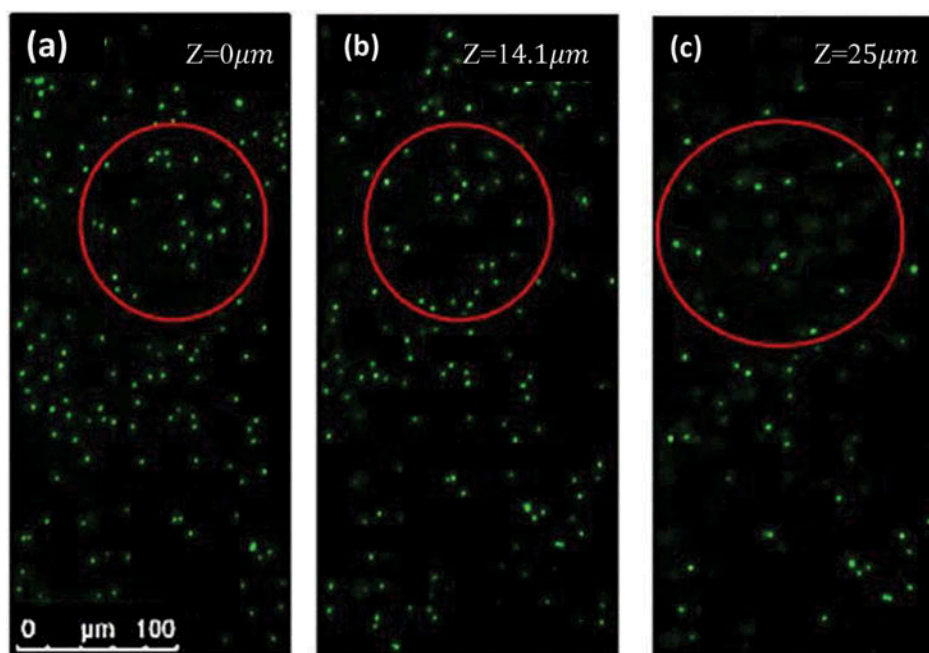


**Figure 2.** Direct microscopic images of alginate gel formation marked with fluorescent polystyrene markers at various distances from NF270 membrane surface,  $t = 15 \text{ min}$ ,  $I_{\text{NaCl}} = 10 \text{ mM}$ ,  $J = 10 \mu\text{m/s}$ . Cross-flow was from left to right at  $6 \text{ cm/s}$ .

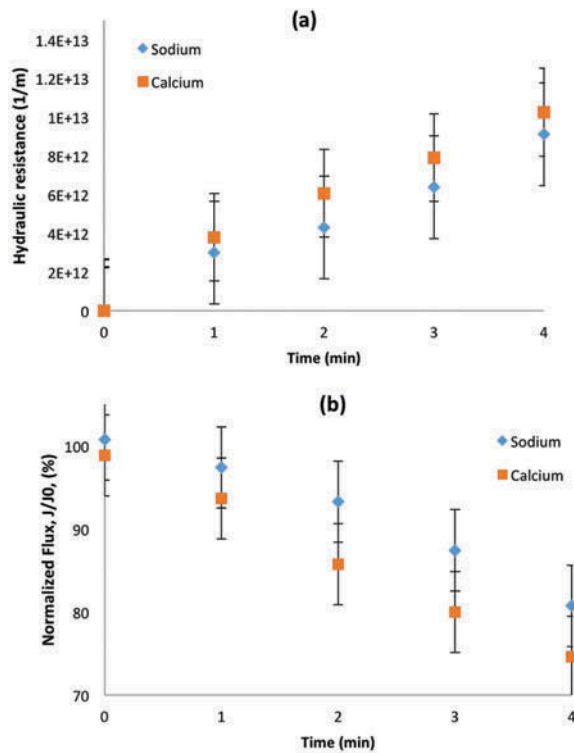


**Figure 3.** (a) Normalized permeate flux decline due to alginate fouling in the presence of 10 mM NaCl or CaCl<sub>2</sub>. (b) The alginate hydraulic resistance versus time in the presence of 10 mM NaCl or CaCl<sub>2</sub>. In these experiments, the water flux was  $J_w = 10 \mu\text{m/s}$ , and the cross-flow velocity was 6 cm/s.

results in substantial permeate flux decline, as shown in Fig. 3a. The effect of calcium and sodium ions' presence on alginate fouling layer resistance is shown in Fig. 3b. It appears that flux decline is more severe in the presence of calcium ions for most of the duration of the fouling experiment. This result is expected, since presence of calcium ions causes the alginate layer to be more rigid – due to calcium bridging, more extensive polymer chain interactions, which results in cross-linking. The hydraulic resistance corresponding with the flux data is shown in Fig. 3b, with a growing resistance of the alginate layer as it builds up; the values measured correspond reasonably well with others reported elsewhere in the literature for bulk alginate deposited at a membrane surface.<sup>[27]</sup> The intrinsic resistance can be expressed as  $r_i = \frac{R_a}{l}$ , where  $R_a$  is the total hydraulic alginate layer resistance and  $l$  is the thickness of the fouling layer. Using the above equation, an estimate of alginate intrinsic resistance was made for the points where layer thicknesses were measured from the microscopy imaging. In the presence of calcium ions, the layer thickness was estimated to be, on average,  $\sim 45 \mu\text{m}$ , putting the intrinsic resistance at  $\sim 2 \times 10^{17} \text{ m}^{-2}$ . It must be noted that in the calculation of the resistance, the effect of concentration polarization present before the addition of alginate was taken into account (accounting for the relative

flux decline due to accumulated salt and the increased osmotic pressure); however, the alginate resistance presented here has a possible compounded effect of “cake-enhanced concentration polarization”, where an enhanced concentration polarization layer is developed due to hindered back-diffusion of the ions and altered cross-flow hydrodynamics within colloidal deposit layers.<sup>[28]</sup>

### Direct observation of alginate detachment

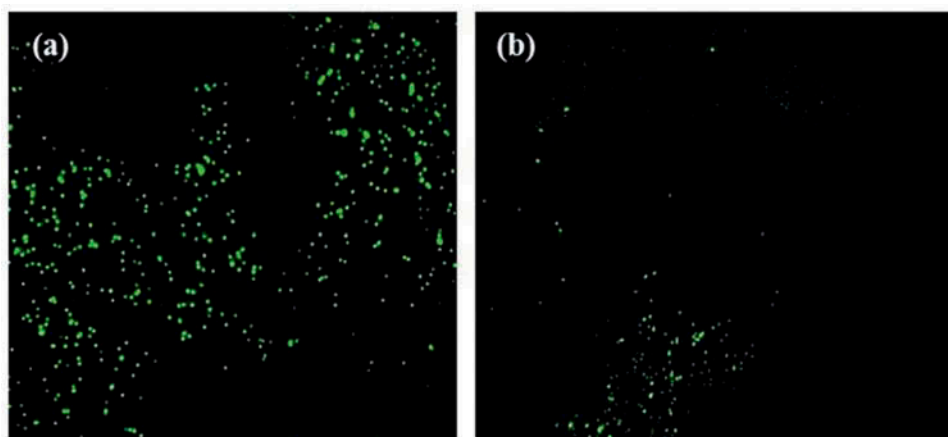
#### Detachment inhomogeneity

Representative images are shown in Fig. 4, taken at random locations on the membrane after a cleaning cycle, which induced alginate detachment. As may be seen, there are locations on the membrane where particles are still largely present (Fig. 4a), while in other locations the membrane appears to be quite clean (Fig. 4b). Analysis of these images showed that particles were located only on the membrane surface (*i.e.* particles were not observed at a distance from the membrane surface), which led to the conclusion that there was no alginate layer left on the membrane. Inhomogeneity of particle detachment may be explained by either the degree of reversibility in the initial deposition, or by an inhomogeneous deposition (very commonly observed for NF270 membranes) – both of these may be due to an uneven flux distribution, due to the membrane composite structure,<sup>[29]</sup> which can lead to uneven deposition and irreversibility.<sup>[30]</sup>

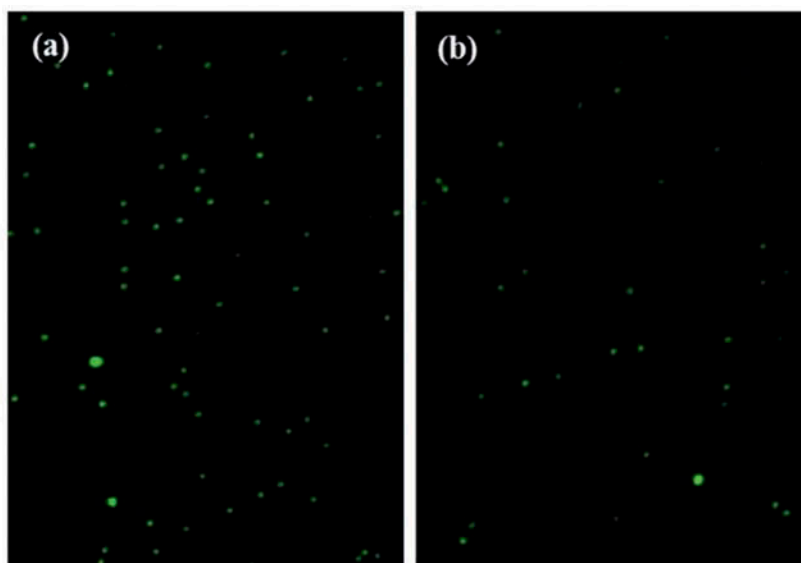
#### Effect of cleaning solution composition on alginate detachment

Figure 5 shows images of the membrane after fouling from an alginate solution containing calcium ions. These images were taken after the first step of the alginate detachment procedure, when the trans-membrane pressure was turned off. Since calcium ions were present, the formed layer is comparatively rigid and resistant to deformations that result from external forces. These conditions are expected to limit the alginate release process that is triggered solely by trans-membrane pressure shut-off. Analysis of these images showed that particles were present at several distances from the membrane, indicating the existence of the alginate layer. Presence of calcium ions indeed made the alginate more resistant to cleaning and reduced detachment efficiency compared with alginate layers formed with only sodium ions present.

In Fig. 6, a sequence is shown from a cleaning cycle in which sodium ions were added (as NaCl) to the calcium-containing feed stream during the cleaning phase, in order to induce ion exchange between



**Figure 4.** Direct microscopic images of in-homogeneities in colloidal and macromolecular detachment,  $I_{\text{NaCl}} = 10\text{mM}$ ,  $\Delta P = 0$  Bar, no flux was measured. Cross-flow was from left to right at 6 cm/s.



**Figure 5.** Direct observation microscopic images of a rigid alginate gel formed in the presence of calcium ions while detachment process was triggered: (a)  $\Delta P = 2.4$  Bar,  $J = 10 \mu\text{m/s}$ ; and (b)  $\Delta P = 0$  Bar, no flux was measured.  $I_{\text{CaCl}_2} = 10$  mM. Cross-flow was from left to right at 6 cm/s.

the deposit and the bulk solution. Figures 6a and 6b show the alginate layer after trans-membrane pressure shut-off, at two locations: the membrane surface and at a distance of  $\sim 40 \mu\text{m}$  from the membrane surface, where static particles were still noticeable. Figures 6c and 6d show the same focal planes after addition of sodium ions. In these images, a clear membrane appears, implying that the alginate layer has now detached completely. Insertion of sodium into the solution displaces some of the calcium out of the alginate deposit, with the sodium taking its place. This ion exchange causes the alginate to become more soft and deformable and it therefore more easily detaches. As already explained, the particles serve as

markers for the presence of alginate since alginate is a transparent substance, and cannot be seen using bright-field or fluorescent microscopy. Therefore, the absence of marker particles leads to the conclusion that all of the alginate was washed away.

### Summary and conclusions

A versatile method is proposed and demonstrated for direct observation of macromolecular fouling and removal, based on the dispersal of fluorescent beads that serve as markers for the presence of an accumulated macromolecular deposit. This method is easy to implement, is generally independent of the fouling substance

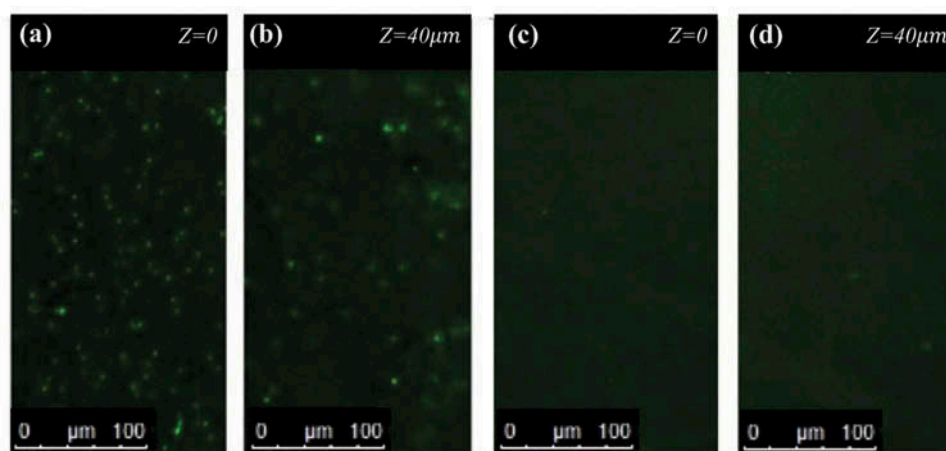


**Figure 6.** Direct observation of alginate gel detachment with presence of calcium ions before sodium ions addition at (a) membrane surface (b) distance of 40  $\mu\text{m}$  from the membrane, and after sodium ions addition at (c) membrane surface and (d) distance of 40  $\mu\text{m}$  from the membrane, Experiment conditions:  $I_{\text{NaCl}} = 10 \text{ mM}$ ,  $I_{\text{CaCl}_2} = 10 \text{ mM}$ ,  $J = 10 \mu\text{m/s}$ . Cross-flow was from left to right at 6 cm/s.

for hydrogel-forming substances typical of bio-fouling and various fluorescent markers can be used. We report the use of alginate as a model for fouling and detachment experiments under direct observation using fluorescent microscopy. Fluorescent markers were added to an alginate solution, and their deposition at various distances from the membrane surface was monitored.

The impact of sodium and calcium ions on alginate detachment was examined. In the absence of calcium, alginate is more deformable and detached relatively easily. The presence of calcium ions forms a rigid alginate gel, and not all of the alginate was detached. After the alginate gel was formed with calcium ions, an addition of sodium ions to the solution causes ion exchange inside the gel, calcium ions diffuse out of the matrix and sodium ions diffuse in. This causes the alginate to lose its strength, facilitating its removal from the membrane.

These processes are used as representative cases whose dynamics may be monitored using the developed method. The proposed method enables real-time examination of a variety of properties, such as fouling layer thickness, with implications on deposition and removal kinetics for various fouling substances. Further refinement is still required and is left for future work. This includes use of confocal microscopy for better resolved cross-sections of the deposited layer, as well as particle-tracking based methods for quantitative estimation of the layer stiffness.

Overall, examination of macromolecular fouling and cleaning using direct observation will allow in-depth studies of mechanisms occurring within deposits at a membrane surface. Such understanding can provide insight crucial for developing efficient cleaning protocols and fouling-resistant membrane surfaces, and may help increase overall separation efficiency.

## Funding

This research was funded by the US-Israel Binational Agricultural R&D fund (BARD) award IS-4768-14R.

## References

- [1] Shannon, M. Bohn, P.W.; Elimelech, M.; Georgiadis, J. G.; Mariñas, B.J.; Mayes, A.M. (2008) Science and technology for water purification in the coming decade. *Nature*, 452: 301–310.
- [2] Semiat, R. (2008) Energy issues in desalination processes. *Environmental Science & Technology*, 42: 8193–8201
- [3] Sonune, A.; Ghate, R. (2004) Developments in wastewater treatment methods. *Desalination* 167: 55–63.
- [4] Guo, W.; Ngo, H.-H.; Li, J.A. (2012) mini-review on membrane fouling. *Bioresource Technology*, 122: 27–34.
- [5] Membrane filtration technologies tackle water reuse and purification. (2007) *Membrane Technology*, 2007: 9–11.
- [6] Lee, S.; Ang, W.S.; Elimelech, M. (2006) Fouling of reverse osmosis membranes by hydrophilic organic matter: implications for water reuse. *Desalination* 187: 313–321.
- [7] Lee, S.; Cho, J.; Elimelech, M. (2005) Combined influence of natural organic matter (NOM) and colloidal particles on nanofiltration membrane fouling. *Journal of Membrane Science*, 262, 27–41.
- [8] Li, H.; Fane, A.G.; Coster, H.G.L.; Vigneswaran, S. (1998) Direct observation of particle deposition on the membrane surface during crossflow microfiltration. *Journal of Membrane Science*, 149: 83–97.
- [9] Li, H.; Fane, A.G. (2000) New insights into membrane operation revealed by direct observation through the membrane. *Membrane Technology*, 2000: 10–14.
- [10] Li, H. (2000) An assessment of depolarisation models of crossflow microfiltration by direct observation through the membrane. *Journal of Membrane Science*, 172: 135–147.
- [11] Mores, W.D.; Davis, R.H. (2002) Direct observation of membrane cleaning via rapid backpulsing. *Desalination* 146: 135–140.

- [12] Mores, W.D.; Davis, R.H. (2002) Yeast foulant removal by backpulses in crossflow microfiltration. *Journal of Membrane Science*, 208: 389–404.
- [13] Li, H.; Fane, A.G.; Coster, H.G.L.; Vigneswaran, S. (2003) Observation of deposition and removal behaviour of submicron bacteria on the membrane surface during crossflow microfiltration. *Journal of Membrane Science*, 217: 29–41.
- [14] Kang, S.; Subramani, A.; Hoek, E.M.V.; Deshusses, M.; Matsumoto, M. (2004) Direct observation of biofouling in cross-flow microfiltration: mechanisms of deposition and release. *Journal of Membrane Science*, 244: 151–165.
- [15] Wang, S.; Guillen, G.; Hoek, E.M.V. (2005) Direct observation of microbial adhesion to membranes. *Environmental Science & Technology*, 39: 6461–6469.
- [16] Subramani, A.; Hoek, E.M.V. (2008) Direct observation of initial microbial deposition onto reverse osmosis and nanofiltration membranes. *Journal of Membrane Science*, 319: 111–125.
- [17] Subramani, A.; Huang, X.; Hoek, E.M.V. (2009) Direct observation of bacterial deposition onto clean and organic-fouled polyamide membranes. *Journal of Colloid and Interface Science*, 336: 13–20.
- [18] Huang, X.; Guillen, G.R.; Hoek, E.M.V. (2010) A new high-pressure optical membrane module for direct observation of seawater RO membrane fouling and cleaning. *Journal of Membrane Science*, 364: 149–156.
- [19] Ang, W.S.; Tiraferri, A.; Chen, K.L.; Elimelech, M. (2011) Fouling and cleaning of RO membranes fouled by mixtures of organic foulants simulating wastewater effluent. *Journal of Membrane Science*, 376: 196–206.
- [20] Kong, H.J.; Wong, E.; Mooney, D.J. (2003) Independent control of rigidity and toughness of polymeric hydrogels. *Macromolecules*, 36 (12): 4582–4588.
- [21] Wan, L.Q.; Jiang, J.; Arnold, D.E.; Guo, X.E.; Lu, H.H.; and Mow, V.C. (2008) Calcium concentration effects on the mechanical and biochemical properties of chondrocyte-alginate constructs. *Cellular and Molecular Bioengineering*, 1: 93–102.
- [22] Wloka, M.; Rehage, H.; Flemming, H.-C.; Wingender, J. (2004) Rheological properties of viscoelastic biofilm extracellular polymeric substances and comparison to the behavior of calcium alginate gels. *Colloid and Polymer Science*, 282: 1067–1076.
- [23] LeRoux, M.A.; Guilak, F.; Setton, L.A. (1999) Compressive and shear properties of alginate gel: effects of sodium ions and alginate concentration. *Journal of Biomedical Materials Research*, 47: 46–53.
- [24] Körstgens, V.; Flemming, H.-C.; Wingender, J.; Borchard, W. (2001) Influence of calcium ions on the mechanical properties of a model biofilm of mucoid *Pseudomonas aeruginosa*. *Water Science and Technology*, 43: 49–57.
- [25] Lee, S.; Elimelech, M. (2007) Salt cleaning of organic-fouled reverse osmosis membranes. *Water Research*, 41: 1134–42.
- [26] Ramon, G.Z.; Nguyen, T.-V.; Hoek, E.M.V. (2013) Osmosis-assisted cleaning of organic-fouled seawater RO membranes. *Chemical Engineering Journal*, 218: 173–182.
- [27] Sioutopoulos, D.C.; Goudoulas, T.B.; Kastrinakis, E. G.; Nychas, S.G.; Karabelas, A.J. (2013) Rheological and permeability characteristics of alginate fouling layers developing on reverse osmosis membranes during desalination, *Journal of membrane science*, 434: 74–84.
- [28] Hoek, E.M.V.; Elimelech, M. (2003) Cake-enhanced concentration polarization: A new fouling mechanism for salt-rejecting membranes. *Environmental Science & Technology*, 37 (24): 5581–5588.
- [29] Ramon, G.Z.; Wong, M.C.Y.; Hoek, E.M.V. (2012) Transport through composite membranes. part 1: Is there an optimal support membrane? *Journal of Membrane Science*, 415–416:298–305.
- [30] Ramon, G.Z.; Hoek, E.M.V. (2012) On the enhanced drag force induced by permeation through a filtration membrane. *Journal of Membrane Science*, 392–393, 1–8.